ISSN 1674-1056
http://cpb.iphy.ac.cn
http://iopscience.iop.org/cpb
中国物理 B
Chinese Physics
中国物理 Chinese Physics B

Acoustic radiation force on a multilayered sphere in a Gaussian standing field

Haibin Wang(汪海宾), Xiaozhou Liu(刘晓宙), Sha Gao(高莎), Jun Cui(崔骏), Jiehui Liu(刘杰惠), Aijun He(何爱军), Gutian Zhang(张古田)
Citation: Chin. Phys. B . 2018, 27(3): 034302. **doi:** 10.1088/1674-1056/27/3/034302

Journal homepage: http://cpb.iphy.ac.cn; http://iopscience.iop.org/cpb

What follows is a list of articles you may be interested in

Random phase screen influence of the inhomogeneous tissue layer on the generation of acoustic vortices

Zhiyao Ma(马致遥), Jun Ma(马骏), Dong Zhang(章东), Juan Tu(屠娟)
Chin. Phys. B . 2018, 27(3): 034301. **doi:** 10.1088/1674-1056/27/3/034301

Acoustic radiation force on a multilayered sphere in a Gaussian standing field

Haibin Wang(汪海宾), Xiaozhou Liu(刘晓宙), Sha Gao(高莎), Jun Cui(崔骏), Jiehui Liu(刘杰惠), Aijun He(何爱军), Gutian Zhang(张古田)
Chin. Phys. B . 2018, 27(3): 034302. **doi:** 10.1088/1674-1056/27/3/034302

Multiple off-axis acoustic vortices generated by dual coaxial vortex beams

Wen Li(李雯), Si-Jie Dai(戴思捷), Qing-Yu Ma(马青玉), Ge-Pu Guo(郭各朴), He-Ping Ding(丁鹤平)
Chin. Phys. B . 2018, 27(2): 024301. **doi:** 10.1088/1674-1056/27/2/024301

Acoustic radiation force induced by two Airy-Gaussian beams on a cylindrical particle

Sha Gao(高莎), Yiwei Mao(毛一葳), Jiehui Liu(刘杰惠), Xiaozhou Liu(刘晓宙)
Chin. Phys. B . 2018, 27(1): 014302. **doi:** 10.1088/1674-1056/27/1/014302

Adaptive optimization on ultrasonic transmission tomography-based temperature image for biomedical treatment

Yun-Hao Zhu(朱昀浩), Jie Yuan(袁杰), Stephen Z Pinter, Oliver D Kripfgans, Qian Cheng(程茜), Xue-Ding Wang(王学鼎), Chao Tao(陶超), Xiao-Jun Liu(刘晓峻), Guan Xu(徐冠), Paul L Carson
Chin. Phys. B . 2017, 26(6): 064301. **doi:** 10.1088/1674-1056/26/6/064301

Acoustic radiation force on a multilayered sphere in a Gaussian standing field*

Haibin Wang(汪海宾)[1], Xiaozhou Liu(刘晓宙)[1,2,†], Sha Gao(高莎)[1], Jun Cui(崔骏)[1], Jiehui Liu(刘杰惠)[1], Aijun He(何爱军)[3], and Gutian Zhang(张古田)[4]

[1] *Key Laboratory of Modern Acoustics, Institute of Acoustics, Nanjing University, Nanjing* 210093, *China*
[2] *State Key Laboratory of Acoustics, Institute of Acoustics, Chinese Academy of Sciences, Beijing* 100190, *China*
[3] *School of Electronic Science and Engineering, Nanjing University, Nanjing* 210023, *China*
[4] *Nanjing Drum Tower Hospital, The Affiliated Hospital of Nanjing University Medical School, Nanjing* 210093, *China*

(Received 27 October 2017; revised manuscript received 5 December 2017; published online 13 February 2018)

We develop a model for calculating the radiation force on spherically symmetric multilayered particles based on the acoustic scattering approach. An expression is derived for the radiation force on a multilayered sphere centered on the axis of a Gaussian standing wave propagating in an ideal fluid. The effects of the sound absorption of the materials and sound wave on acoustic radiation force of a multilayered sphere immersed in water are analyzed, with particular emphasis on the shell thickness of every layer, and the width of the Gaussian beam. The results reveal that the existence of particle trapping behavior depends on the choice of the non-dimensional frequency *ka*, as well as the shell thickness of each layer. This study provides a theoretical basis for the development of acoustical tweezers in a Gaussian standing wave, which may benefit the improvement and development of acoustic control technology, such as trapping, sorting, and assembling a cell, and drug delivery applications.

Keywords: acoustic radiation force, Gaussian standing field, multilayered sphere model, sound scattering

PACS: 43.25.Qp, 43.35.Wa, 43.80.Gx **DOI:** 10.1088/1674-1056/27/3/034302

1. Introduction

In recent years, many theoretical and experimental studies have been performed on the acoustic radiation force exerted by a single ultrasonic beam on spherical objects.[1–9] The acoustic tweezers based on acoustic radiation force have become a well-known technique for trapping, sorting, and assembling microparticles (guiding and trapping minuscule particles).[4–13] In particular, in cellular and molecular biology, particle manipulation has been crucial in studying biomechanical properties of various cells and molecules. However, most of these particles mentioned in previous papers are single-layered spherical shell structures. In biomedical engineering and materials science, there are many particles with multiple-layered structures, for example, nanoparticle drugs and cells. In drug delivery applications,[14–17] using acoustic radiation can effectively manipulate polymer microspheres filled with liquid drugs, such that the shell is accurately broken and the drugs can be used in affected areas. A common cell is typically a multilayered tissue that contains a cell membrane, cytoplasm, and a cell nucleus. The acoustic properties of these layers are different; therefore, the study of acoustic radiation force on multilayered spherical shell structures has practical value for applications.

An acoustic standing field can be useful in microfluidic lab-on-a-chip applications, and researchers have calculated the radiation force function for plane and Bessel standing waves.[18–24] A Gaussian standing beam has been used to develop acoustic tweezers that can immobilize latex particles and frog eggs in a fixed position.[25] In this paper, we present a model to calculate the acoustic radiation force by a Gaussian standing wave upon a spherically symmetric multilayered sphere based on previous research.[11,26,27] Examples for the radiation force on two- and three-layered spheres with isotropic properties in each layer are studied for the radius ratio of different layered materials. This study shows that the theory developed in this paper provides a theoretical basis for multilayered spherical particle manipulation.

2. Theory

2.1. Expansion of incident Gaussian standing wave in terms of spherical functions

Let a Gaussian standing wave be incident upon a three-layered sphere immersed in an inviscid fluid medium, with the wave propagating along the $+z$ direction. The origin of coordinates of the spherical coordinate system is shown in Fig. 1. The center position of the sphere is the origin of coordinates,

*Project supported by National Key R&D Program of China (Grant No. 2016YFF0203000), the National Natural Science Foundation of China (Grant Nos. 11774167 and 61571222), the Fundamental Research Funds for the Central Universities of China (Grant No. 020414380001), the Key Laboratory of Underwater Acoustic Environment, Institute of Acoustics, Chinese Academy of Sciences (Grant No. SSHJ-KFKT-1701), and the AQSIQ Technology R&D Program of China (Grant No. 2017QK125).

†Corresponding author. E-mail: xzliu@nju.edu.cn

© 2018 Chinese Physical Society and IOP Publishing Ltd

which is at distance h from each beam waist of a Gaussian standing wave field, where a, b, and c are the outer, mid, and inner radii of a spherically symmetric three-layered sphere.

For simplicity, it is assumed that the Gaussian beam is weakly focused. Moreover, the phase front of propagation of the Gaussian beam is almost equal to the plane wave near the beam waist. This means that it can be approximately regarded as an acoustic wave with Gaussian amplitude distribution in that region. Assume also a homogeneous and isotropic fluid of infinite extent with adiabatic speed of sound c_1 and density ρ_1. The velocity potential of the incident sound wave can be written as [11]

$$\phi_i = \phi_0 \mathrm{e}^{-(x^2+y^2)/W_0^2}\left(\mathrm{e}^{\mathrm{i}k(z+h)} + \mathrm{e}^{-\mathrm{i}k(z+h)}\right)\mathrm{e}^{-\mathrm{i}\omega t}, \quad (1)$$

where ϕ_0 is the amplitude of the incident velocity potential, W_0 is the width of the Gaussian beam, k is the wavenumber, and ω is the angular frequency of the wave.

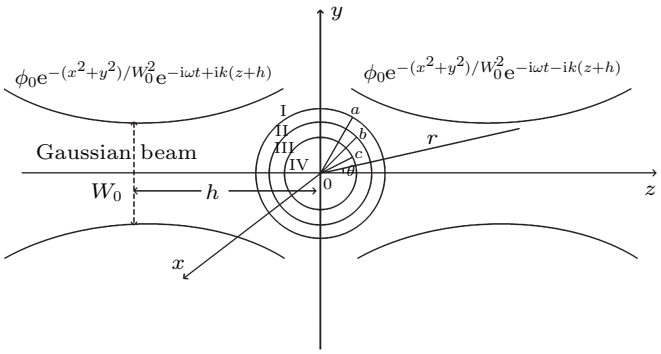


Fig. 1. Coordinate geometry of the Gaussian standing wave and a three-layered sphere model.

Let $x = r\sin\theta\cos\varphi$, $y = r\sin\theta\sin\varphi$, $z = r\cos\theta$, $s = 1/kW_0$, $\rho_1 = kr$.

In a spherical coordinate system, the velocity potential of an incident wave can be expressed in terms of a general eigenfunction expansion of the form[8,18]

$$\phi_i = \phi_0 \sum_{n=0}^{\infty} \delta_n Q_n \mathrm{i}^n (2n+1) j_n(\rho) \mathrm{P}_n(\cos\theta)\exp(-\mathrm{i}\omega t), \quad (2)$$

where

$$\delta_n = \left(\mathrm{e}^{\mathrm{i}kh} + (-1)^n \mathrm{e}^{-\mathrm{i}kh}\right), \quad (3)$$

$$Q_{2n} = \frac{\Gamma(n+1)}{\Gamma(n+1/2)} \sum_{j=0}^{n} \frac{\Gamma(n+j+1/2)}{\Gamma(n-j)!\,j!} \times \left(-4s^2\right)^j, \quad (4)$$

$$Q_{2n+1} = \frac{\Gamma(n+1)}{\Gamma(n+3/2)} \sum_{j=0}^{n} \frac{\Gamma(n+j+3/2)}{\Gamma(n-j)!\,j!} \times \left(-4s^2\right)^j, \quad (5)$$

$j_n(\cdot)$ is a spherical Bessel function of order n, $\mathrm{P}_n(\cdot)$ is a Legendre function of order n, and $\Gamma(\cdot)$ is the gamma function. From Eqs. (4) and (5), the beam coefficients Q_n can be determined by the dimensionless parameter $1/kW_0$. The convergent items are different for different ratios of W_0 to λ.

To validate the finite series method, the incident Gaussian beam has been calculated by exact solution as well as a finite series solution for different beam widths.[4] The results show that when $W_0 \geq 2\lambda$, the wave beam computed by a finite series is in agreement with the exact solution.[8]

2.2. Scattering of a Gaussian standing wave by three-layered spherical particles

The Gaussian standing wave with wavelength λ_1 in an infinite medium is scattered by the sphere. Assume that the incident wave is axisymmetric, and the outer fluid water has density ρ_1 and sound speed c_1. In spherical coordinates, the velocity potential of the incident wave can be expressed in terms of a general eigenfunction expansion of the form shown in Eq. (2).

The scattered velocity potential can be expressed as

$$\phi_s = \phi_0 \sum_{n=0}^{\infty} \delta_n Q_n \mathrm{i}^n (2n+1) A_n h_n^{(1)}(k_1 r) \times \mathrm{P}_n(\cos\theta)\exp(-\mathrm{i}\omega t), \quad (6)$$

where $h_n^{(1)}(\cdot)$ is the Hankel function of the first kind, and A_n is the unknown scattering coefficient, which is to be determined by the boundary conditions. Therefore, the total scalar velocity potential outside the sphere can be written as

$$\phi_1 = \phi_i + \phi_s = \phi_0 \sum_{n=0}^{\infty} \delta_n Q_n \mathrm{i}^n (2n+1)\left(j_n(k_1 r) + A_n h_n^{(1)}(k_1 r)\right)\mathrm{P}_n(\cos\theta)\exp(-\mathrm{i}\omega t). \quad (7)$$

The particle vector displacement U_i ($i = 2, 3, 4$) in the shell of the elastic material is assumed to be[2,3]

$$\boldsymbol{U}_i = -\boldsymbol{\nabla}\boldsymbol{\Phi}_i + \boldsymbol{\nabla}\times\boldsymbol{\Psi}_i, \quad (8)$$

where the scalar potential Φ_i and the vector potential $\boldsymbol{\Psi}_i$ ($\Psi_{ir} = 0, \Psi_{i\theta} = 0, \Psi_{i\varphi}$) can be expanded in series by using the unknown coefficients B_n, C_n, D_n, E_n, F_n, G_n, H_n, I_n, K_n, L_n, respectively, as follows:

$$\Phi_2 = \phi_0 \sum_{n=0}^{\infty} \delta_n Q_n (2n+1)\mathrm{i}^n \left(B_n j_n(k_{21}r) + C_n n_n(k_{21}r)\right) \times \mathrm{P}_n(\cos\theta)\exp(-\mathrm{i}\omega t), \quad (9)$$

$$\Psi_{2\varphi} = \phi_0 \sum_{n=0}^{\infty} \delta_n Q_n (2n+1)\mathrm{i}^n \left(D_n j_n(k_{22}r) + E_n n_n(k_{22}r)\right) \times \frac{\mathrm{d}\mathrm{P}_n(\cos\theta)}{\mathrm{d}\theta}\exp(-\mathrm{i}\omega t), \quad (10)$$

$$\Phi_3 = \phi_0 \sum_{n=0}^{\infty} \delta_n Q_n (2n+1)\mathrm{i}^n \left(F_n j_n(k_{31}r) + G_n n_n(k_{31}r)\right) \times \mathrm{P}_n(\cos\theta)\exp(-\mathrm{i}\omega t), \quad (11)$$

$$\Psi_{3\varphi} = \phi_0 \sum_{n=0}^{\infty} \delta_n Q_n (2n+1)\mathrm{i}^n \left(H_n j_n(k_{32}r) + I_n n_n(k_{32}r)\right) \times \frac{\mathrm{d}\mathrm{P}_n(\cos\theta)}{\mathrm{d}\theta}\exp(-\mathrm{i}\omega t), \quad (12)$$

$$\Phi_4 = \phi_0 \sum_{n=0}^{\infty} \delta_n Q_n (2n+1) \mathrm{i}^n K_n j_n(k_{41} r) \times \mathrm{P}_n(\cos\theta) \exp(-\mathrm{i}\omega t), \quad (13)$$

$$\Psi_{4\varphi} = \phi_0 \sum_{n=0}^{\infty} \delta_n Q_n (2n+1) \mathrm{i}^n L_n j_n(k_{42} r) \times \frac{\mathrm{d}\mathrm{P}_n(\cos\theta)}{\mathrm{d}\theta} \exp(-\mathrm{i}\omega t), \quad (14)$$

where $n_n(\cdot)$ is a spherical Bessel function of the second kind, and $k_{21}(k_{31}, k_{41})$ and $k_{22}(k_{32}, k_{42})$ are the wave numbers of the longitudinal and shear waves, respectively. In the shell material (medium 2, 3, 4), B_n, C_n, D_n, E_n, F_n, G_n, H_n, I_n, K_n, L_n are the unknown coefficients determined by the boundary conditions.

The boundary conditions lead to 11 linear equations. After laborious but straightforward calculations, the scattering coefficient A_n is determined in the following form:

$$A_n = \frac{\begin{vmatrix} b_1 & q_{12} & q_{13} & q_{14} & q_{15} & 0 & 0 & 0 & 0 & 0 & 0 \\ b_2 & q_{22} & q_{23} & q_{24} & q_{25} & 0 & 0 & 0 & 0 & 0 & 0 \\ 0 & q_{32} & q_{33} & q_{34} & q_{35} & 0 & 0 & 0 & 0 & 0 & 0 \\ 0 & q_{42} & q_{43} & q_{44} & q_{45} & q_{46} & q_{47} & q_{48} & q_{49} & 0 & 0 \\ 0 & q_{52} & q_{53} & q_{54} & q_{55} & q_{56} & q_{57} & q_{58} & q_{59} & 0 & 0 \\ 0 & q_{62} & q_{63} & q_{64} & q_{65} & q_{66} & q_{67} & q_{68} & q_{49} & 0 & 0 \\ 0 & q_{72} & q_{73} & q_{74} & q_{75} & q_{76} & q_{77} & q_{78} & q_{79} & 0 & 0 \\ 0 & 0 & 0 & 0 & 0 & q_{86} & q_{87} & q_{88} & q_{89} & q_{810} & q_{811} \\ 0 & 0 & 0 & 0 & 0 & q_{96} & q_{97} & q_{98} & q_{99} & q_{910} & q_{911} \\ 0 & 0 & 0 & 0 & 0 & q_{106} & q_{107} & q_{108} & q_{109} & q_{1010} & q_{1011} \\ 0 & 0 & 0 & 0 & 0 & q_{116} & q_{117} & q_{118} & q_{119} & q_{1110} & q_{1111} \end{vmatrix}}{\begin{vmatrix} q_{11} & q_{12} & q_{13} & q_{14} & q_{15} & 0 & 0 & 0 & 0 & 0 & 0 \\ q_{12} & q_{22} & q_{23} & q_{24} & q_{25} & 0 & 0 & 0 & 0 & 0 & 0 \\ 0 & q_{32} & q_{33} & q_{34} & q_{35} & 0 & 0 & 0 & 0 & 0 & 0 \\ 0 & q_{42} & q_{43} & q_{44} & q_{45} & q_{46} & q_{47} & q_{48} & q_{49} & 0 & 0 \\ 0 & q_{52} & q_{53} & q_{54} & q_{55} & q_{56} & q_{57} & q_{58} & q_{59} & 0 & 0 \\ 0 & q_{62} & q_{63} & q_{64} & q_{65} & q_{66} & q_{67} & q_{68} & q_{49} & 0 & 0 \\ 0 & q_{72} & q_{73} & q_{74} & q_{75} & q_{76} & q_{77} & q_{78} & q_{79} & 0 & 0 \\ 0 & 0 & 0 & 0 & 0 & q_{86} & q_{87} & q_{88} & q_{89} & q_{810} & q_{811} \\ 0 & 0 & 0 & 0 & 0 & q_{96} & q_{97} & q_{98} & q_{99} & q_{910} & q_{911} \\ 0 & 0 & 0 & 0 & 0 & q_{106} & q_{107} & q_{108} & q_{109} & q_{1010} & q_{1011} \\ 0 & 0 & 0 & 0 & 0 & q_{116} & q_{117} & q_{118} & q_{119} & q_{1110} & q_{1111} \end{vmatrix}}, \quad (15)$$

where b_i and q_{ij} are the dimensionless elements of the determinants given in Appendix A.

2.3. Acoustic radiation force on a layered spherical shell

The acoustic radiation force $\langle \boldsymbol{F} \rangle$ on a boundary moving with a velocity of the first order was calculated by Yosioka and Kawasima[28] as

$$\langle \boldsymbol{F} \rangle = -\iint_{S(t)} \langle P - \mathrm{P}_0 \rangle \boldsymbol{n} \,\mathrm{d}S == -\left\langle \iint \rho (v_\mathrm{n} \boldsymbol{n} + v_\mathrm{t} \boldsymbol{t}) v_\mathrm{n} \,\mathrm{d}S \right\rangle + \left\langle \iint \frac{1}{2} \rho_1 v^2 \boldsymbol{n} \,\mathrm{d}S \right\rangle - \left\langle \iint \frac{1}{2} \frac{\rho_1}{c_1^2} \left(\frac{\partial \phi_1}{\partial t} \right)^2 \boldsymbol{n} \,\mathrm{d}S \right\rangle, \quad (16)$$

where S is the boundary at its equilibrium position, v_n and v_t are the normal and tangential components of the particle velocity of the boundary, respectively, and the symbol $\langle \cdot \rangle$ denotes time averaging.

After calculation, $\langle F \rangle$ can be expressed as

$$\langle F \rangle = \pi a^2 E Y_\mathrm{P} \sin(2kh) \quad (17)$$

and

$$Y_\mathrm{P} = -\frac{8}{(ka)^2} \sum_{n=0}^{\infty} (n+1)(-1)^{(n+1)} \times \left\{ \mathrm{Re}[Q_n Q_{n+1}^*] [\beta_{n+1}(1+2\alpha_n) - \beta_n (1+2\alpha_n)] - \mathrm{Im}[Q_n Q_{n+1}^*] [\alpha_n + \alpha_{n+1} + 2\alpha_n \alpha_{n+1} + 2\beta_n \beta_{n+1}] \right\}, \quad (18)$$

where Y_P is a dimensionless factor called the radiation force function, $*$ denotes the complex conjugate, and α_n and β_n are the real and imaginary parts of the scattering coefficients A_n defined by Eq. (15).

3. Numerical calculation of Y_P and analysis

The acoustic radiation force function Y_P given by Eq. (18) is evaluated for multilayered spheres, of which the physical constants are assumed as listed in Table 1. In this paper, we mainly discuss the two-layered and three-layered microsphere model shown in Figs. 2 and 3, respectively. Two 30-MHz Gaussian ultrasonic transducers are used for simulation, which means the wavelength of ultrasound in water is 50 μm. For the acoustic scattering approach to be valid, the wavelength of ultrasound should be greater than or approximately equal to the size of an object; thus, the radius of sphere in the simulation is smaller than 50 μm. The detailed analyses regarding acoustic radiation force acting on the microspheres are presented as follows.

Table 1. The physical constants of materials used in the sample calculations.[11,29,30]

Materials	Mass density /10^3 kg·m^{-3}	Compressional velocity/m·s^{-1}	Shear velocity/m·s^{-1}	Normalized longitudinal absorption γ_{21}	Normalized shear absorption γ_{22}
Water	1.00	1500	…	…	…
Animal oil	0.80	1400	…	…	…
Stainless steel	7.90	5240	2978	…	…
Polyethylene	0.957	2430	950	0.0073	0.022
Polymethyl methacrylate	1.19	2690	1340	0.0035	0.0053

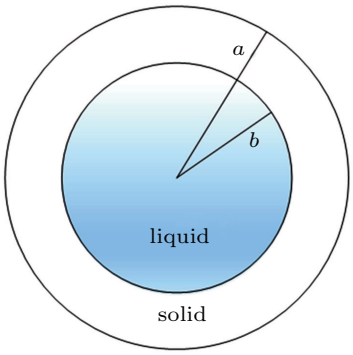


Fig. 2. (color online) Two-layered sphere model.

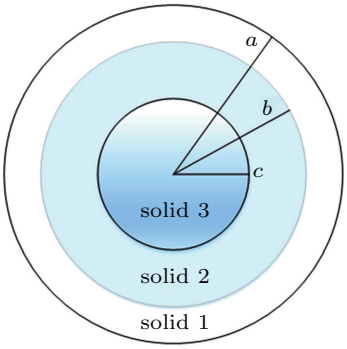


Fig. 3. (color online) Three-layered sphere model.

3.1. Two-layered polymer-coated liquid sphere model

The acoustic radiation force acting on a fluid drug coated by a spherical polymer-type layer can be used for drug delivery applications in which the shell is accurately broken and the drug is used in the affected areas. The plots of axial radiation forces in a two-layered model ($e_1 = b/a$, $c = 0$) of low density polymethyl methacrylate (PMMA) shell filled with water and animal oil are shown in Figs. 4–8.

Figure 4 shows the radiation force function Y_P vs. ka for a PMMA sphere shell filled with water in a Gaussian standing wave at $W_0 = 5a$ with different e_1 ($e_1 = b/a$) values. The simulation results indicate that the curves have a series of prominent peaks and dips, which are caused by the effects of resonant vibration of the PMMA sphere shell. The magnitudes of the resonant peaks and dips decrease with an increase of ka value. Moreover, the peaks and dips change with different value of e_1, which illustrates the thickness of inner and outer layers of the sphere affecting the resonance frequencies of the model.

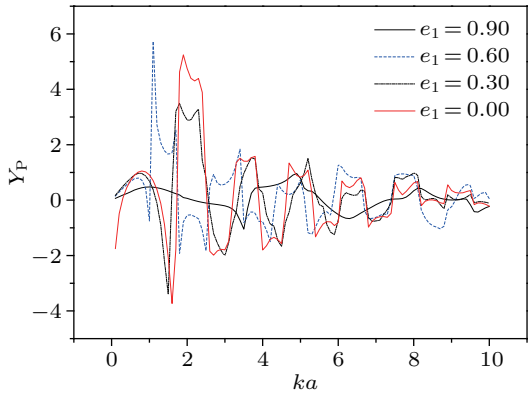


Fig. 4. (color online) Acoustic radiation force function vs. ka for the two-layered sphere filled with water with different e_1.

In addition, with a large difference on acoustic impedance between the PMMA shell and the surrounding medium (water), the particle suffers larger radiation force when $e_1 = b/a = 0$ (the sphere becomes a single-layered PMMA sphere, and the numerical result is in agreement with the results of Wu[6]). With an increase of the inner radius, the negative acoustic radiation force becomes smaller and smaller, and then disappears, and the radiation force decreases and approaches zero in the situation of a thin shell with a further increase of the inner radius.

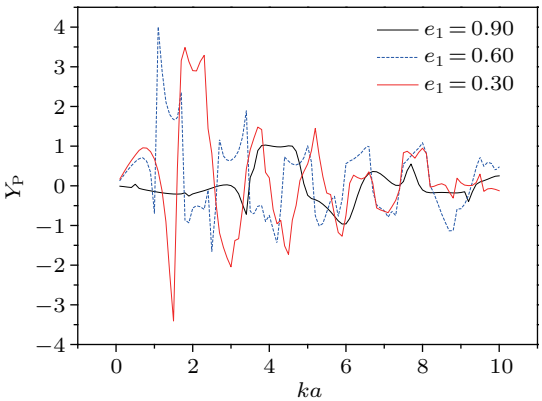


Fig. 5. (color online) Acoustic radiation force function vs. ka for the two-layered sphere filled with animal oil with different e_1.

Figure 5 shows the radiation force function Y_P vs. ka for a PMMA sphere shell filled with animal oil in a Gaussian stand-

ing wave at $W_0 = 5a$ with $e_1 = 0.90$, $e_1 = 0.60$, and $e_1 = 0.30$, respectively. The Y_P-ka curves also have a series of prominent peaks and dips for cases of shell structure where $0 < ka < 10$. Moreover, from comparative analysis, a difference between Figs. 4 and 5 can be easily found because of the difference in the physical properties of the two inner materials.

Figures 6 and 7 show the radiation force function for different beam widths of the Gaussian standing wave at $e_1 = 0.90$. The width of the Gaussian standing wave influences the radiation force function. The magnitudes of the peaks and the dips increase along with the increasing W_0. When the beam waist is far greater than the radius of the sphere ($W_0 > 5a$), the radiation force function of the Gaussian standing beam approaches that of a plane standing wave. Similar results have been presented in the literature, where the acoustic radiation force of the Gaussian beam approaches that of a plane wave at $W_0 > 5a$ for a single sphere.[9]

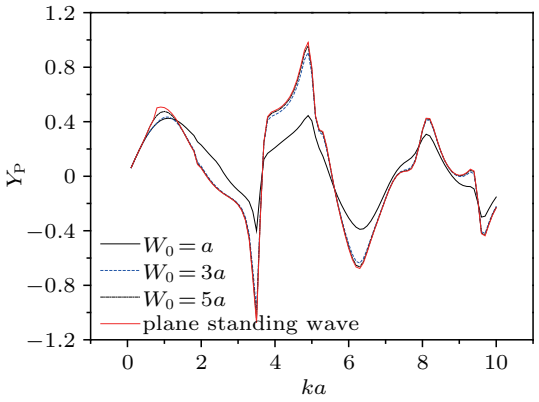


Fig. 6. (color online) Acoustic radiation force function vs. ka for the two-layered sphere filled with water with different W_0.

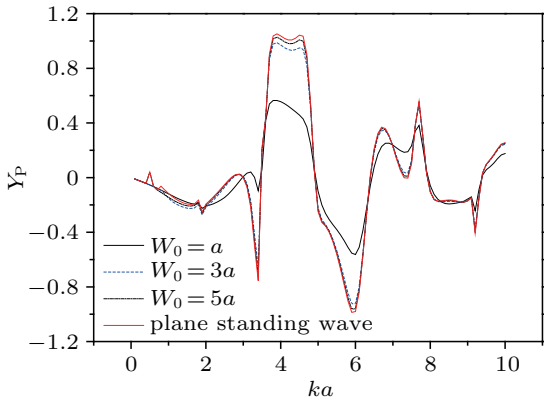


Fig. 7. (color online) Acoustic radiation force function vs. ka for the two-layered sphere filled with animal oil with different W_0.

Figure 8 shows the radiation force function for the two-layered sphere, considering the sound absorption of the polymeric material. As shown in the figure, Y_P decreases with the magnitudes of the peaks and dips in each curve. Therefore, the absorption of sound is an important factor for the acoustic radiation force.

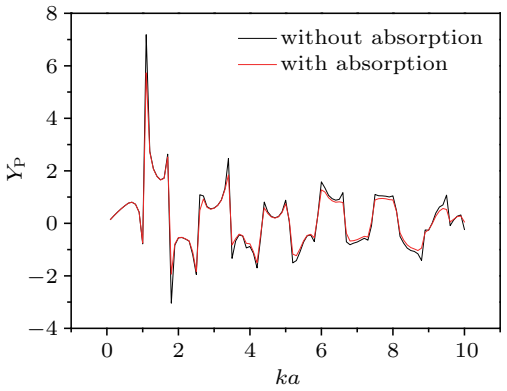


Fig. 8. (color online) Acoustic radiation force function vs. ka for a two-layered sphere filled with water, considering the sound absorption of the polymeric material.

3.2. Three-layered solid sphere model

Relative to the single-layered and two-layered spherical structures, many biological tissues have a three-layered spherical structure. Hence, the study of acoustic radiation force on three-layered spherical shell structures has more practical value for applications. Figures 9–11 show the simulation results for a three-layered solid sphere model, where PMMA, polyethylene, and stainless steel are chosen as the materials for the three-layered structure in the simulation.

In Fig. 9, the Y_P–ka curves are computed in the Gaussian standing wave at $W_0 = 5a$, and $e_2 = c/a = 0.60$, for different values for e_1. It is found that the acoustic radiation force fluctuates significantly and decreases with an increase of ka. However, the Y_P-ka curves have no significant change with the thickness of the materials for the outermost and middle layers, which can be explained by noting that PMMA and polyethylene have similar physical properties.

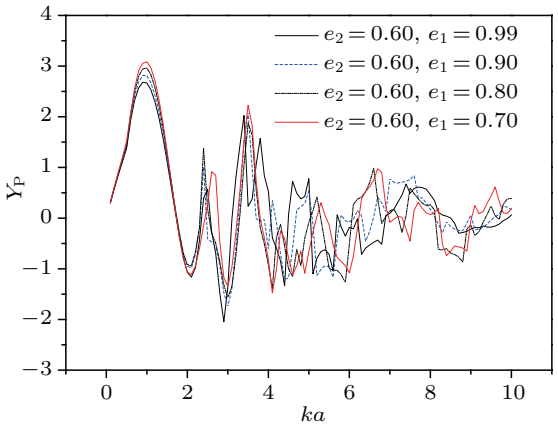


Fig. 9. (color online) Acoustic radiation force function vs. ka for a three-layered sphere with different e_1.

Figure 10 shows the radiation force function Y_P in the Gaussian standing wave at $W_0 = 5a$, and $e_1 = 0.90$, for different values of e_2. From the simulation results, the acoustic radiation force function has a series of prominent peaks and dips. In addition, the numerical values depend on the value of e_2. From the above analyses, it can be concluded that the

values of e_2 (the thickness of each layer) have an effect on the radiation force function. When the acoustic impedance of two adjacent materials is very different, the values of e_2 can have a huge effect on the acoustic radiation force.

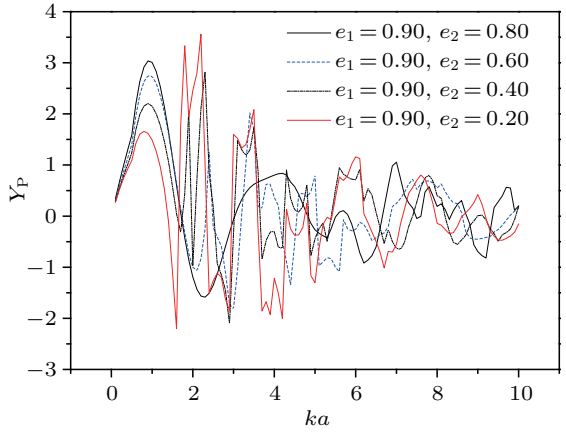


Fig. 10. (color online) Acoustic radiation force function vs. ka for the three-layered sphere with different e_2.

Figure 11 shows that the radiation force changes with the width of the Gaussian standing wave at $e_1 = 0.90$, $e_2 = 0.60$. Similar with Figs. 6 and 7, the width of the Gaussian standing wave influences the radiation force function. The magnitudes of the peaks and the dips increase with the increasing W_0. When the beam waist is far greater than the radius of the sphere, the radiation force function of the Gaussian standing beam approaches that of a plane standing wave.

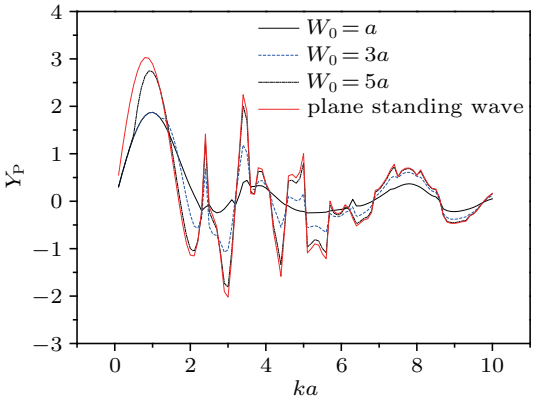


Fig. 11. (color online) Acoustic radiation force function vs. ka for the three-layered sphere with different W_0.

4. Conclusions

Based on the finite series method, the Gaussian standing wave using spherical harmonic functions and the beam coefficients of the Gaussian beam are observed. The acoustic radiation force function can be obtained for a multilayered spherical particle in fluid using the Gaussian standing wave acoustic field. The numerical analyses for two- and three-layered spherical shells are performed with a particular emphasis on the effects of the ratio of outer radius to inner radius of the shell on the acoustic radiation force. We also discuss the influence of the width of the Gaussian wave on the radiation force function. The results show that the acoustic radiation force is negative at some ka values, generating a potential well. This suggests the possibility of using Gaussian standing waves to manipulate multilayered spheres with known mechanical and acoustical properties, providing an impetus for further research on cell biomechanics and drug delivery. However, if further progress can be made in the structure of a cell and drug carrier microsphere, such as the acoustical properties of cell components, more valuable and meaningful results can be obtained based on the theory presented in this paper.

Appendix A

Let ρ_1, ρ_2, ρ_3, ρ_4 be the mass densities of regions I, II, III, and IV, respectively; $e_1 = b/a$, $e_2 = c/a$ where a, b, and c are the outer, middle, and inner radii (Fig. 1); $x_1 = k_1 a$, $x_{21} = x_1 c_1(1+\mathrm{i}\gamma_{21})/c_{21}$, $x_{22} = x_1 c_1(1+\mathrm{i}\gamma_{22})/c_{22}$, $x_{31} = x_1 c_1(1+\mathrm{i}\gamma_{31})/c_{31}$, $x_{32} = x_1 c_1(1+\mathrm{i}\gamma_{32})/c_{32}$, $x_{41} = x_1 c_1/c_{41}$, $x_{42} = x_1 c_1/c_{42}$, $y_{21} = x_{21}e$, $y_{22} = x_{22}e$, $y_{31} = x_{31}e$, $y_{32} = x_{32}e$, $z_{31} = x_{31}f$, $z_{32} = x_{32}f$, $z_{41} = x_{41}f$, and $z_{42} = x_{42}f$, where $k_1 = \omega/c_1$, c_1 is the sound velocity in water, c_{21} and c_{22} are the compressional and shear sound velocities in the outer layer, γ_{21} and γ_{22} are their corresponding absorption coefficients; c_{31} and c_{32} are the compressional and shear sound velocities in the middle material, γ_{31} and γ_{32} are their corresponding absorption coefficients (Table 1); and $\mu_i = \rho_i c_{i2}^2$, $\lambda_i = \rho_i c_{i1}^2 - 2\mu_i$, where μ_i, λ_i are lame coefficients of the corresponding medium ($i = 2,3,4$).

The following terms are the expressions for the elements of the determinants appearing in Eq. (15):

$$
\begin{aligned}
b_1 &= x_1 j_n'(x_1),\\
b_2 &= -\frac{\rho_1}{\rho_2} x_{22}^2 j_n(x_1),\\
q_{11} &= -x_1 h_n^{(1)\prime}(x_1),\\
q_{12} &= x_{21} j_n'(x_{21}),\\
q_{13} &= x_{21} n_n'(x_{21}),\\
q_{14} &= -n(n+1) j_n(x_{22}),\\
q_{15} &= -n(n+1) n_n(x_{22}),\\
q_{21} &= \frac{\rho_1}{\rho_2} x_{22}^2 h_n^{(1)}(x_1),\\
q_{22} &= 2x_{21}^2 j_n''(x_{21}) - (x_{22}^2 - 2x_{21}^2) j_n(x_{21}),\\
q_{23} &= 2x_{21}^2 n_n''(x_{21}) - (x_{22}^2 - 2x_{21}^2) n_n(x_{21}),\\
q_{24} &= 2n(n+1)(j_n(x_{22}) - x_{22} j_n'(x_{22})),\\
q_{25} &= 2n(n+1)(n_n(x_{22}) - x_{22} n_n'(x_{22})),\\
q_{32} &= 2(x_{21} j_n'(x_{21}) - j_n(x_{21})),\\
q_{33} &= 2(x_{21} n_n'(x_{21}) - n_n(x_{21})),\\
q_{34} &= (2 - n^2 - n) j_n(x_{22}) - x_{22}^2 j_n''(x_{22}),
\end{aligned}
$$

$$q_{35} = (2-n^2-n)n_n(x_{22}) - x_{22}^2 n_n''(x_{22}),$$
$$q_{42} = y_{21} j_n'(y_{21}),$$
$$q_{43} = y_{21} n_n'(y_{21}),$$
$$q_{44} = -n(n+1) j_n(y_{22}),$$
$$q_{45} = -n(n+1) n_n(y_{22}),$$
$$q_{46} = -y_{31} j_n'(y_{31}),$$
$$q_{47} = -y_{31} n_n'(y_{31}),$$
$$q_{48} = n(n+1) j_n(y_{32}),$$
$$q_{49} = n(n+1) n_n(y_{32}),$$
$$q_{52} = j_n(y_{21}),$$
$$q_{53} = n_n(y_{21}),$$
$$q_{54} = -y_{22} j_n'(y_{22}) - j_n(y_{22}),$$
$$q_{55} = -y_{22} n_n'(y_{22}) - n_n(y_{22}),$$
$$q_{56} = -j_n(y_{31}),$$
$$q_{57} = n_n(y_{31}),$$
$$q_{58} = y_{32} j_n'(y_{32}) + j_n(y_{32}),$$
$$q_{59} = y_{32} n_n'(y_{32}) + n_n(y_{32}),$$
$$q_{62} = 2\mu_2 y_{21}^2 j_n''(y_{21}) - \lambda_2 y_{21}^2 j_n(y_{21}),$$
$$q_{63} = 2\mu_2 y_{21}^2 n_n''(y_{21}) - \lambda_2 y_{21}^2 n_n(y_{21}),$$
$$q_{64} = 2\mu_2 n(n+1)(j_n(y_{22}) - y_{22} j_n'(y_{22})),$$
$$q_{65} = 2\mu_2 n(n+1)(n_n(y_{22}) - y_{22} n_n'(y_{22})),$$
$$q_{66} = -2\mu_3 y_{31}^2 j_n''(y_{31}) + \lambda_3 y_{31}^2 j_n(y_{31}),$$
$$q_{67} = -2\mu_3 y_{31}^2 n_n''(y_{31}) + \lambda_3 y_{31}^2 n_n(y_{31}),$$
$$q_{68} = 2\mu_3 n(n+1)(y_{32} j_n'(y_{32}) - j_n(y_{32})),$$
$$q_{69} = 2\mu_3 n(n+1)(y_{32} n_n'(y_{32}) - n_n(y_{32})),$$
$$q_{72} = 2\mu_2(y_{21} j_n'(y_{21}) - j_n(y_{21})),$$
$$q_{73} = 2\mu_2(y_{21} n_n'(y_{21}) - n_n(y_{21})),$$
$$q_{74} = (2-n^2-n)\mu_2 j_n(y_{22}) - \mu_2 y_{22}^2 j_n''(y_{22}),$$
$$q_{75} = (2-n^2-n)\mu_2 n_n(y_{22}) - \mu_2 y_{22}^2 n_n''(y_{22}),$$
$$q_{76} = 2\mu_3(j_n(y_{31}) - y_{31} j_n'(y_{31})),$$
$$q_{77} = 2\mu_3(n_n(y_{31}) - y_{31} n_n'(y_{31})),$$
$$q_{78} = (n^2+n-2)\mu_3 j_n(y_{32}) + \mu_3 y_{32}^2 j_n''(y_{32}),$$
$$q_{79} = (n^2+n-2)\mu_3 n_n(y_{32}) + \mu_3 y_{32}^2 n_n''(y_{32}),$$
$$q_{86} = z_{31} j_n'(z_{31}),$$
$$q_{87} = z_{31} n_n'(z_{31}),$$
$$q_{88} = -n(n+1) j_n(z_{32}),$$
$$q_{89} = -n(n+1) n_n(z_{32}),$$
$$q_{810} = -z_{41} j_n'(z_{41}),$$
$$q_{811} = n(n+1) j_n(z_{42}),$$
$$q_{96} = j_n(z_{31}),$$
$$q_{97} = n_n(z_{31}),$$
$$q_{98} = -z_{32} j_n'(z_{32}) - j_n(z_{32}),$$
$$q_{99} = -z_{32} n_n'(z_{32}) - n_n(z_{32}),$$
$$q_{910} = -j_n(z_{41}),$$
$$q_{911} = z_{42} j_n'(z_{42}) + j_n(z_{42}),$$
$$q_{106} = 2\mu_3 z_{31}^2 j_n''(z_{31}) - \lambda_3 z_{31}^2 j_n(z_{31}),$$
$$q_{107} = 2\mu_3 z_{31}^2 n_n''(z_{31}) - \lambda_3 z_{31}^2 n_n(z_{31}),$$
$$q_{108} = 2\mu_3 n(n+1)(j_n(z_{32}) - z_{32} j_n'(z_{32})),$$
$$q_{109} = 2\mu_3 n(n+1)(n_n(z_{32}) - z_{32} n_n'(z_{32})),$$
$$q_{1010} = -2\mu_4 z_{41}^2 j_n''(z_{41}) + \lambda_4 z_{41}^2 j_n(z_{41}),$$
$$q_{1011} = 2\mu_4 n(n+1)(z_{42} j_n'(z_{42}) - j_n(z_{42})),$$
$$q_{116} = 2\mu_3(z_{31} j_n'(z_{31}) - j_n(z_{31})),$$
$$q_{117} = 2\mu_3(z_{31} n_n'(z_{31}) - n_n(z_{31})),$$
$$q_{118} = (2-n^2-n)\mu_3 j_n(z_{32}) - \mu_3 z_{32}^2 j_n''(z_{32}),$$
$$q_{119} = (2-n^2-n)\mu_3 n_n(z_{32}) - \mu_3 z_{32}^2 n_n''(z_{32}),$$
$$q_{1110} = 2\mu_4(j_n(z_{41}) - z_{41} j_n'(z_{41})),$$
$$q_{1111} = (n^2+n-2)\mu_4 j_n(z_{42}) + \mu_4 z_{42}^2 j_n''(z_{42}),$$

References

[1] Wu R and Du G H 1990 *J. Acoust. Soc. Am.* **87** 997
[2] Hasegawa T and Yosioka K 1969 *J. Acoust. Soc. Am.* **46** 1139
[3] Hasegawa T, Hino Y, Annou A, Noda H and Kato M 1993 *J. Acoust. Soc. Am.* **93** 154
[4] Lee J W, Ha K L and Shung K K 2005 *J. Acoust. Soc. Am.* **117** 3273
[5] Lee J W, Lee C Y and Shung K K 2010 *IEEE Trans. Ultrason. Ferroelectr. Freq. Control* **57** 2305
[6] Lee J W 2011 *Biotechnology and Bioengineering* **108** 1643
[7] Ying L and Shung K K 2013 *Appl. Phys. Lett.* **102** 084102
[8] Zhang X F, Song Z G and Chen D M 2015 *J. Acoust. Soc. Am.* **137** 1826
[9] Zhang X F and Zhang G B 2012 *Ultrasound Med. Biol.* **38** 2007
[10] Huang X Y, Yan C F, Cheng L W, Rong Z H and Jian H Z 2017 *Acta Phys. Sin.* **66** 044301 (in Chinese)
[11] Wu R R, Cheng K X, Liu X Z, Liu J H, Gong X F and Li Y F 2016 *Wave Motion* **62** 63
[12] Shi J J, Ahmed D and Mao X L 2009 *Lab. Chip.* **9** 2861
[13] Li S, Ding X, Guo F, Chen Y and Lapsley M 2013 *Anal. Chem.* **85** 5468
[14] Brannon-Peppas L 1997 *Medical plastics and biomaterials* **4** 34
[15] Hu Y, Qin S and Jiang Q 2004 *IEEE Trans. UFFC* **51** 808
[16] Cain C, Jeffers R, Feng R Q and Fowlkes B 1992 *International Conference of the IEEE Engineering in Medicine & Biology Society* **1** 356
[17] Munshi N, Rapoport N and Pitt W G 1997 *Cancer Lett.* **118** 13
[18] Hasegawa T 1979 *J. Acoust. Soc. Am.* **65** 32
[19] Shi J J, Ahmed D and Mao X L 2009 *Lab. Chip.* **9** 2861
[20] Li S, Ding X, Guo F, Chen Y and Lapsley M 2013 *Anal. Chem.* **85** 5468
[21] Chen Y C 2014 *Lab. Chip.* **14** 916
[22] Mitri F G 2007 *Arch. Appl. Mech.* **77** 1
[23] Mitri F G 2008 *Ann. Phys.* **323** 1604
[24] Mitri F G 2009 *Ultrasonics* **49** 794
[25] Wu J R 1991 *J. Acoust. Soc. Am.* **89** 2140
[26] Mitri F G 2005 *Eur. Phys. J. B* **43** 379
[27] Wang Y Y, Yao J, Wu X W and Wu D 2017 *J. Appl. Phys.* **122** 094902
[28] Yoshioka K and Kawashima Y 1955 *Acustica* **5** 167
[29] Norris A N 2017 *J. Acoust. Soc. Am.* **141** 475
[30] Hartmann B 10.1002/app.1975.0701912111975 *J. Appl. Polym. Sci.* **12** 3241